

Superconducting shells in ceramic $\text{YBa}_2\text{Cu}_3\text{O}_7$

D. S. Ginley, E. L. Venturini, J. F. Kwak, R. J. Baughman, B. Morosin, and J. E. Schirber

Sandia National Laboratories, P.O. Box 5800, Albuquerque, New Mexico 87185

(Received 6 April 1987; revised manuscript received 11 May 1987)

We demonstrate that, even in single-phase ceramic $\text{YBa}_2\text{Cu}_3\text{O}_7$, superconductivity occurs in only thin shells surrounding normal grains. The shells comprise no more than 25 vol% of the material, independent of preparation technique and subsequent processing. This conclusion is based on comparison of magnetic-flux exclusion, Meissner and resistivity data for bulk, compacted, and ground materials. We show that these data depend on the sample microstructure, but do not arise from pinning effects.

The observation of superconductivity with onset temperatures as high as 97 K for yttrium barium copper oxides¹⁻⁴ has stimulated tremendous interest in the nature of the superconductivity in these materials. In this paper we demonstrate that *even in single-phase* ceramic $\text{YBa}_2\text{Cu}_3\text{O}_7$ ("1-2-3" material), and for a wide range of processing conditions, superconductivity occurs only in thin shells surrounding normal grains. All relevant experimental techniques demonstrate that our "1-2-3" material is comparable to the best reported to date.⁵⁻¹⁰ We will discuss in order the synthesis protocols and morphology for all samples, then the data for bulk ceramics, compacted materials, and finally powders. All data support the existence of the shells.

Bulk ceramic "1-2-3" material was synthesized from mixtures of CuO , BaO , and Y_2O_3 or of CuO , Y_2O_3 , and BaCO_3 , and also from mixed oxides that were made by drying (14 h at 140°C) and calcining (2 h at 825°C in air) homogeneously coprecipitated carbonates generated by dripping sodium carbonate into a solution of the elemental nitrates up to pH 9.5. All of the powders were ground, pelletized at 5.6 kbar, and sintered in air for 4 h at 900°C (sintering in oxygen gave less satisfactory results). Samples were then oxygen annealed (640–700 Torr) under a variety of conditions including (1) 900°C for 12 h, (2) 900°C for 12–60 h with a 5 h slow cool, (3) 500°C for 55 h with a 5 h slow cool, and (4) 900°C for 12 h followed by 500°C for 5 h with a 5 h slow cool. Materials from (2) and (4) had the best superconducting properties, but oxygen anneals longer than 12 h at 900°C were not beneficial. Densities ranged from 50% to 80% of the theoretical value, 6.5 g/cm³. Some materials were compacted in air to 100% density between stainless steel or WC dies at 20–30 kbar after all other processing. Powders of controlled particle size were prepared by grinding with an agate mortar and pestle and sieving through standard meshes. X-ray powder patterns of all the above materials indicated single-phase material with all observed lines accounted for by an orthorhombic unit cell of $a_0 = 3.825$, $b = 3.883$, and $c = 11.680$ Å.

Figure 1 shows scanning electron microscopy (SEM) photomicrographs of the mixed oxide material before and after high-pressure compaction and of homogeneously coprecipitated material. Mixed oxide material has blocky grains with a range of sizes averaging 10 μm. Homogeneously

coprecipitated material has a uniform network of connected rods about 10-μm long and 2–4-μm across. Compacted material from ground powders or bulk shows evidence of plastic flow. Energy-dispersive x ray shows both the mixed oxides and coprecipitated materials to be very uniform in composition.

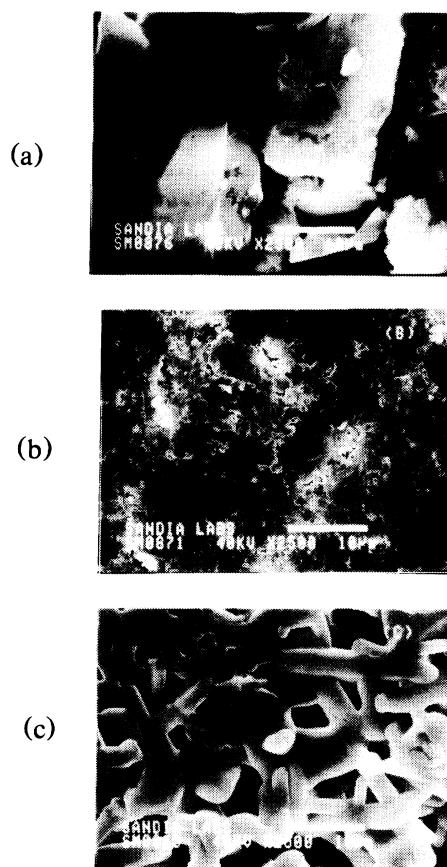


FIG. 1. Scanning electron micrographs of processed $\text{YBa}_2\text{Cu}_3\text{O}_7$. (a) Sintered and oxygen annealed mixed oxide material exhibiting large irregular grains; (b) same preparation as in (a) but then compacted to approximately 25 kbar in air; (c) sintered and oxygen annealed homogeneously coprecipitated material exhibiting a porous network of rodlike grains. All pictures at 2500X, and the bar is 10 μm.

The static magnetization for all materials was measured in a commercial superconducting quantum interference device magnetometer (Biomagnetic Technologies, San Diego, CA). Solid samples were suspended as thin rectangular plates parallel to the applied magnetic field to minimize demagnetization corrections; powders were held in a cylindrical plastic bucket. Flux exclusion (diamagnetic shielding) was determined by cooling to 5 K in nearly zero field and then applying the measurement field and warming the sample. Flux expulsion (Meissner effect) was obtained by cooling in the measurement field. Flux expulsion of mixed oxide material at 5 K gives a susceptibility of $-0.006 \text{ cm}^3/\text{g}$, or $-4\pi\chi = 0.49$ using theoretical density. A similar Meissner value has been reported recently.⁵ Low-frequency ac resistivity of solid samples was measured using a quasilinear four-probe configuration, and the current density was kept low enough to avoid any effects on the shape of the transition.

Figure 2 shows static magnetization versus temperature for a bulk mixed oxide "1-2-3" sample in an applied magnetic field of 0.25 mT. Curve A (solid circles) shows flux exclusion and curve B (open triangles) shows flux expulsion for the sample. Note, in particular, the step in the exclusion data starting at 88 K (shown in more detail in the inset). The shape of these two curves is similar to those published elsewhere.^{5,9,10} However, the details of the flux exclusion and Meissner data near T_c have not been examined previously.

The difference between the flux expulsion and flux exclusion data is central to our model for this ceramic material; each grain has a nonsuperconducting interior surrounded by a thin superconducting shell. In curve A, this shell excludes flux from the entire grain until the penetration depth approaches the shell thickness. Above 80 K, flux exclusion drops sharply as the applied field penetrates through the superconducting shell. While the shells remain superconducting to 93 K, the step at 88 K indicates that the penetration depth has exceeded the shell thickness. The relative size and onset temperature of the

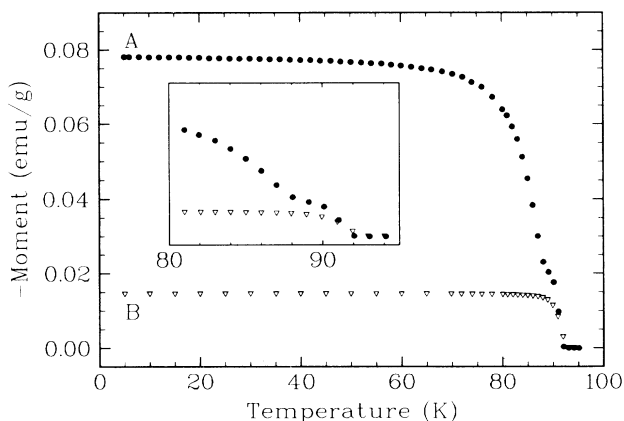


FIG. 2. Flux exclusion warming data (solid circles) and flux expulsion cooling data (open triangles) in 0.25 mT for a mixed oxide pellet of $\text{YBa}_2\text{Cu}_3\text{O}_7$. Inset shows superconducting onset near 93 K and step in warming data near 88 K.

step is independent of applied field between 0.1 and 1 mT. In the expulsion experiments flux is trapped in the nonsuperconducting grain interiors and is expelled only from the superconducting shells. The temperature independence of the magnetization data below 80 K indicates that the shell thickness greatly exceeds the penetration depth.

From the ratio of flux expulsion to flux exclusion, we can estimate the volume fraction of superconducting material to be 0.18 to 0.25 for mixed oxide material and 0.15 to 0.18 for the more uniform coprecipitated material. Using the approximation of 10- μm -diam spherical grains from the SEM data, this volume fraction corresponds to shell thicknesses of 0.30 to 0.45 μm for mixed oxides and 0.3 μm for the coprecipitated material. The origin and thickness of the shells may be related to the heterogeneity of the starting materials or the effects of strain, local ordering, or the effective partial pressure of the reactants during processing. Mixed-phase samples such as $\text{Y}_{1.2}\text{Ba}_{0.8}\text{CuO}_4$ (Ref. 1) show exclusion-to-expulsion ratios as large as 30:1 rather than the 4 or 5:1 observed in single-phase "1-2-3" material.

For a sample of bulk mixed oxide "1-2-3" material, curve A in Fig. 3 shows resistivity data. The transition width, resistivity ratio, and $R=0$ point at 91 K compare favorably with results reported elsewhere.⁵⁻¹⁰ This sharp transition requires a highly interconnected network of shells.

Bulk materials were compacted at high pressures because the ensuing plastic flow should break the shells, exposing the normal grain interiors. In contrast to the bulk data in Fig. 2, the compacted samples have the same diamagnetic onset temperature, but the flux exclusion and flux expulsion values are in close agreement. At 5 K in 0.25 mT the exclusion is -0.014 emu/g , and the expulsion is -0.012 emu/g . Note that both values are in good agreement with the expulsion result in Fig. 2, confirming that compaction has broken all the shells. These results preclude pinning as an explanation for the large difference between the curves in Fig. 2, since the highly defective

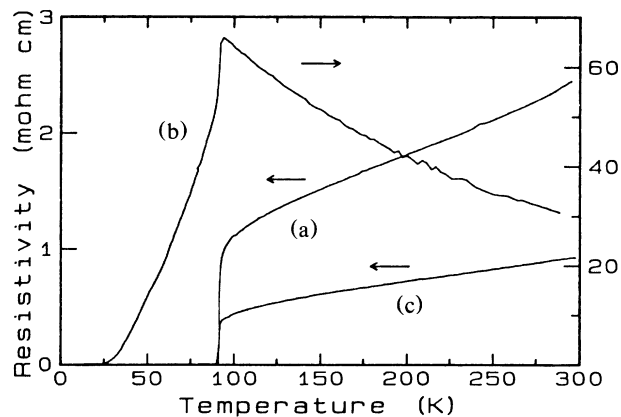


FIG. 3. Resistivity vs temperature for (a) mixed oxide $\text{YBa}_2\text{Cu}_3\text{O}_7$ material, (b) the same as (a) but compacted, and (c) the same as (b) reannealed in oxygen. Arrows refer to the vertical axes.

compacted material should show more pinning and therefore a greater exclusion to expulsion ratio than that for bulk samples.

Resistive data for a compacted mixed oxide are shown in curve B of Fig. 3. The transition is greatly smeared with $R=0$ suppressed to 20 K. A current density of 0.2 A/cm^2 further suppresses $R=0$ to below 10 K, consistent with percolation through a poorly connected network of superconducting shell fragments. Oxygen annealing this material [using protocol (2) above] recreates the interconnects and restores the original transition as shown in curve C.

The compacted material (curve B) has a much higher resistivity and a nonmetallic temperature dependence above 100 K, reminiscent of that reported for quenched "1-2-3" material.⁹ Potential microprobe measurements¹¹ on compacted material at 295 K indicate that the grains are still metallic, with large potential drops observed at stress-induced faults in the microstructure. These results indicate that the grain interiors are metallic in all of the "1-2-3" materials.

Compacted materials after oxygen anneal showed partial recovery of flux exclusion (-0.040 emu/g at 5 K in 0.25 mT for a mixed oxide sample) and little change in flux expulsion. This indicates that the recreated interconnects, observed resistively, also restore diamagnetic shielding, but that oxygen anneals alone are not sufficient to create additional superconducting shells. This may have important ramifications for the synthesis of these materials.

As shown in Table I, sieved powders from ground mixed oxide or coprecipitated bulk "1-2-3" material have a flux exclusion at 5 K that decreases monotonically with decreasing particle size. Upon prolonged grinding, the exclusion falls to a final value which does not change with additional grinding and approaches the expulsion value in bulk material (or the expulsion and exclusion value in compacted material). As the material is ground, some shells get broken, exposing the nonsuperconducting grain interiors and decreasing the flux exclusion. Prolonged grinding fractures all of the shells, producing a result analogous to that from the compaction experiments. The flux expulsion for heavily ground powders is 70% of the exclusion value at 5 K in sharp contrast to the ratio in bulk samples.

Highly ground powders were compacted, and the exclusion value was unchanged, showing that the grinding results were not due to packing of the particles. Heavily ground powder was reannealed in oxygen [protocol (2) above] and showed no change in exclusion or expulsion. Since annealing should remove defects introduced by

TABLE I. Effect of particle size on flux exclusion at 5 K in a 0.25-mT applied field for ground metal oxide and coprecipitated $\text{YBa}_2\text{Cu}_3\text{O}_7$ materials.

Particle size (μm)	Mixed oxide magnetization (emu/g)	Coprecipitate magnetization (emu/g)
Bulk	-0.078	-0.063
> 300	-0.066	-0.060
150-300	-0.060	-0.054
75-150	-0.057	-0.045
37-75	-0.051	-0.040
20-37	-0.049	-0.034
< 20	-0.045	-0.033
< 20 ^a	-0.024	-0.016

^aAfter very heavy grinding for 5 min (all other powders lightly ground).

grinding, such defects do not play a role in the grinding data. Mechanistically the inability to restore shells in ground powder may indicate that grain-to-grain contacts are necessary to form the superconducting shells.

In conclusion, single-phase "1-2-3" material, synthesized by a variety of techniques and processed under a wide range of conditions, appears to consist of interconnected grains composed of a metallic center surrounded by superconducting shells. This model explains the detailed magnetization and resistance data from bulk ceramic, compacted, and ground samples. The thickness of the shells and the morphology of the material is controlled by the synthetic method employed and the nature of the subsequent processing. Intergrain contacts are required for efficient shell formation. Superconducting shells may be intrinsic to these materials, or a different approach to material processing may yield a bulk single-phase superconductor. The fact that shells are always observed may have important ramifications with regard to the mechanism of the superconductivity in these materials as well as their practical utility. One consequence of the shells may be low critical currents. These questions are currently being addressed.

We take pleasure in acknowledging Dr. Carl Seager and Dr. Kent Schubert for the potential microprobe measurements, and R. Hellmer, M. Mitchell, T. Castillo, and D. Overmeyer for their expert technical assistance. This work was performed at Sandia National Laboratories, supported by the U.S. Department of Energy under Contract No. DE-AC04-76DP00789.

¹M. K. Wu, J. R. Ashburn, C. J. Torng, P. H. Hor, R. L. Meng, L. Gao, Z. J. Huang, Y. Q. Wang, and C. W. Chu, *Phys. Rev. Lett.* **58**, 908 (1987).

²H. Takagi, S. Uchida, K. Kishio, K. Kitazawa, K. Fueki, and S. Tanaka, *Jpn. J. Appl. Phys.* **26**, L320 (1987).

³J. Z. Sun, D. J. Webb, M. Naito, K. Char, M. R. Hahn, J. W. P. Hsu, A. D. Kent, D. B. Mitzi, B. Oh, M. R. Beasley, T. H. Geballe, R. H. Hammond, and A. Kapitulnik, *Phys. Rev. Lett.* **58**, 1574 (1987).

⁴J. M. Tarascon, L. H. Greene, W. R. McKinnon, and G. W. Hull, *Phys. Rev. B* **35**, 7115 (1987).

⁵R. J. Cava, B. Batlogg, R. B. van Dover, D. W. Murphy, S. Sunshine, T. Siegrist, J. P. Remeika, E. A. Reitman, S. Zahurak, and G. P. Espinosa, *Phys. Rev. Lett.* **58**, 1676 (1987).

⁶D. W. Murphy, S. Sunshine, R. B. van Dover, R. J. Cava, B. Batlogg, S. M. Zahurak, and L. F. Schneemeyer, *Phys. Rev. Lett.* **58**, 1888 (1987).

- ⁷P. H. Hor, R. L. Meng, Y. Q. Wang, L. Gao, Z. J. Huang, J. Bechtold, K. Forster, and C. W. Chu, *Phys. Rev. Lett.* **58**, 1891 (1987).
- ⁸K. Kadowaki, Y. K. Huang, M. van Sprang, and A. A. Menovsky, *Physica B* **145**, 1 (1987).
- ⁹P. M. Grant, R. B. Beyers, E. M. Engler, G. Lim, S. S. P. Parkin, M. L. Ramirez, V. Y. Lee, A. Nazzal, J. E. Vazquez, and R. J. Savoy, *Phys. Rev. B* **35**, 7242 (1987).
- ¹⁰W. J. Gallagher, R. L. Sandstrom, T. R. Dinger, T. M. Shaw, and D. A. Chance (unpublished).
- ¹¹E. L. Venturini, D. S. Ginley, R. J. Baughman, C. H. Seager, W. K. Schubert, J. F. Kwak, J. E. Schirber, and B. Morosin (unpublished).

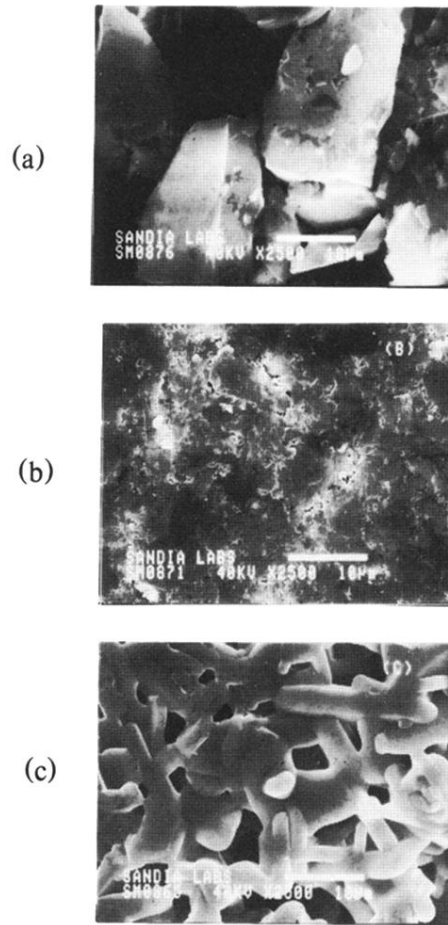


FIG. 1. Scanning electron micrographs of processed $\text{YBa}_2\text{Cu}_3\text{O}_7$. (a) Sintered and oxygen annealed mixed oxide material exhibiting large irregular grains; (b) same preparation as in (a) but then compacted to approximately 25 kbar in air; (c) sintered and oxygen annealed homogeneously coprecipitated material exhibiting a porous network of rodlike grains. All pictures at 2500X, and the bar is 10 μm .